

Accurate Corrections of HPGe Detector Efficiency for NAA Samples

Nader M. A. Mohamed*

Atomic Energy Authority, ETRR-2, 13759 Abou Zabal, Cairo, Egypt

Received: 2 Feb. 2017, Revised: 2 Apr. 2017, Accepted: 26 Apr. 2016

Published online: 1 May 2017

Abstract: In this paper, different methods to correct HPGe detector full-energy peak efficiency for Neutron Activation Analysis (NAA) samples are presented. These methods include Monte Carlo method and analytical formulas. An analytical formula for the sample geometry correction has been derived. A comparison between the Monte Carlo and analytical calculations results were performed. The experiment carried out in this research showed that the Monte Carlo method and the derived formula are highly accurate methods for HPGe detector full-energy peak efficiency corrections for NAA samples.

Keywords: HPGe detector; Full-energy peak efficiency; Corrections; NAA samples.

1 Introduction

The accuracy of Neutron Activation Analysis (NAA) technique depends on the accuracy of the data used in all the NAA stages. Most current NAA laboratories operate HPGe detectors for the radioactivity analyses. HPGe detectors usually are calibrated using standard sources that are available as small deposits on thin backing material so that they may closely approximate non absorbing point sources. Although, NAA samples are usually very small (~500 mg), the effect of sample geometry and gamma-ray self-attenuation on the detector efficiency would not be neglected for accurate NAA results.

Monte Carlo method is widely used for the evaluation of the efficiencies of the HPGe detectors [1-3]. Usually, the Monte Carlo method is used to find a correction factor F for correcting the full-energy peak efficiency of the detector, calibrated by point sources, for volume samples [4-6]:

$$\mathcal{E}_s = F \mathcal{E}_p, \tag{1}$$

where, \mathcal{E}_s is the detector efficiency for the sample and \mathcal{E}_p is the detector efficiency for the point source. In this case the detector calibration is simulated for the point source and for the sample of interest and the correction factor F would be:

$$F = \frac{\mathcal{E}_{sC}}{\mathcal{E}_{pC}}, \tag{2}$$

where, \mathcal{E}_{sC} is the calculated detector efficiency for the sample and \mathcal{E}_{pC} is the calculated detector efficiency for the

point source. This method eliminates the error regarding the uncertainty in the detector data (e.g. detector’s window thickness, active and inactive Ge dimensions,...) and the accuracy will depend on the accuracy of the simulation of the sample.

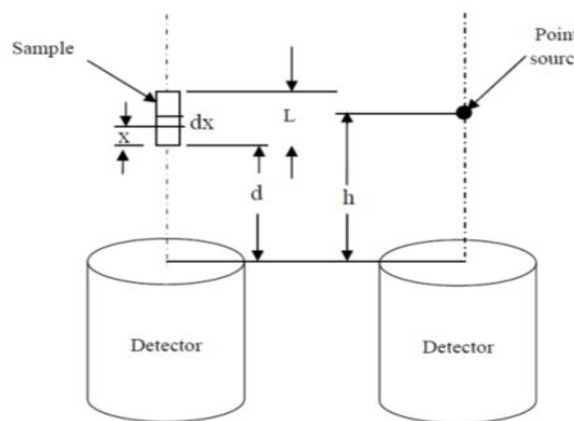


Figure 1. Schematic diagram of sample-detector configuration.

In the analytical methods for HPGe detector full-energy peak efficiency corrections, the correction factor F is usually unfolded to two correction factors:

$$F = F_G F_\mu, \tag{3}$$

where, F_G is the sample geometry correction and F_μ is sample self-attenuation correction. The common way of evaluating F_G is by correcting the solid angle covered by the detector from a point source to the sample [7-9]. In

*Corresponding author e-mail: mnader73@yahoo.com

particular, Aguiar et al. [8] has generated the following geometric correction factor for cylindrical samples:

$$F_G = \frac{2}{3L} \left[L - r \arctan\left(\frac{d+L}{r}\right) + \frac{(d+L)^3}{2r^2} \ln\left(1 + \frac{r^2}{(d+L)^2}\right) + r \arctan\left(\frac{d}{r}\right) - \frac{d^3}{2r^2} \ln\left(1 + \frac{r^2}{d^2}\right) \right], \quad (4)$$

where, L is the sample height, d is the distance between the sample and the detector crystal and r is the sample radius. Eq. (4) correct the detector efficiency calibrated by a point source located at the position of the sample center ($h = d + L/2$, Figure 1).

The simple method of calculating the gamma-ray self-attenuation correction is by assuming a parallel radiation emission [10,11]. In this case, the relative number of photons emitted from an element, dx (Figure 1) that penetrate a distance x before leaving the sample towards the detector is:

$$e^{-\mu x},$$

where, μ is the linear attenuation coefficient. For a homogeneous distribution of the radioactivity in the sample, the fraction of gamma photons emitted from the element dx is:

$$dx/L$$

Therefore, the attenuation correction factor will be:

$$F_\mu = \int_0^L \frac{e^{-\mu x} dx}{L} = \frac{1 - e^{-\mu L}}{\mu L} \quad (5)$$

The accuracy of this formula depends on the sample size, the attenuation coefficient (which depends on the photon energy) and the distance between the sample and the detector.

The last correction factor that should be considered, in particular when low photon energy is considered is the container wall attenuation of gamma-ray, F_w . Assuming parallel radiation emission, this correction would be:

$$F_w = e^{-\mu_w t}, \quad (6)$$

where, μ_w is the attenuation coefficient of the container wall and t is the wall thickness.

The aim of this paper is to present different methods to correct HPGe detector full-energy peak efficiency for NAA samples including Monte Carlo method and analytical formulas. A simple formula for the geometry correction factor, F_G considering the NAA samples would be derived. The validity of the derived formula and the sample self attenuation correction given by Eq. (5) would be studied, as well.

2 Geometry Correction

Assuming NAA cylindrical samples, the geometry correction factor, F_G would depend on the sample diameter and the sample length. Although in the geometry factor

calculations, sample is assumed to be vacuum, this factor is also depends on the photon energy. This is due to that the angular distribution of photons incident on the detector window differs from a point source to a volume source.

The Monte Carlo code: MCNPX [12] was used to calculate the geometry correction factor for an HPGe detector exposed to a disk source at different photon energies. The detector diameter and height are 8 cm and 10 cm, respectively ($8^D \times 10^H$ cm). Two disk diameters were considered: 2 and 8 cm and two positions for each were simulated: at 0.5 and 10 cm from the detector crystal. Pulse height distribution tally, F8 with corresponding E8 tally were used to record the photons which deposited all their energies in the detector. The uncertainties in the results were around 0.2%. The results are plotted as given in Figure 2. The dependence of F_G on the photon energy appears clearly from the results of the large disk diameter. Therefore, the dependence of F_G on the photon energy should not be ignored for bulk samples especially when it is counted on (or near) the detector window.

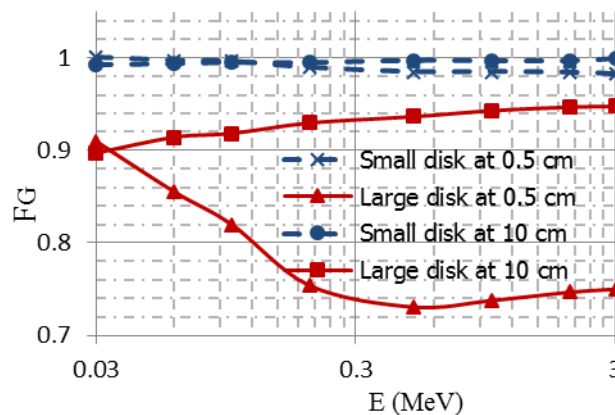


Figure 2. Geometry factors as function of the photon energy for an $8^D \times 10^H$ cm HPGe detector exposed to 2 and 8 cm diameter disk sources at 0.5 and 10 cm from the detector crystal.

In the case of small disk, F_G is very close to 1. In this study, the NAA samples are considered to be had small diameters with respect to detector diameter such that a disk sample correction, $F_G \sim 1$. Three cases were treated to study the geometry correction factor for small disks sources as function of the detector diameters and their positions with respect to the detector crystal. These cases are:

1. An $8^D \times 10^H$ cm HPGe detector exposed to 2 cm diameter disk source.
2. An $8^D \times 10^H$ cm HPGe detector exposed to 1 cm diameter disk source.
3. An $4^D \times 6^H$ cm HPGe detector exposed to 1 cm diameter disk source.

The calculations were carried out at photon energy of 1 MeV. Figure 3 shows F_G of the three cases as function of the source position. NAA samples diameters usually are

less than 1 or 2 cm and usually are measured far enough from the detector to avoid the coincidences. As shown in Figure 3, the effect of the sample diameter on the detector efficiency can be ignored when the samples are counted at a distance higher than 5 or 7 cm from the detector crystal. In this case the sample height has the dominant effect on the geometry correction factor.

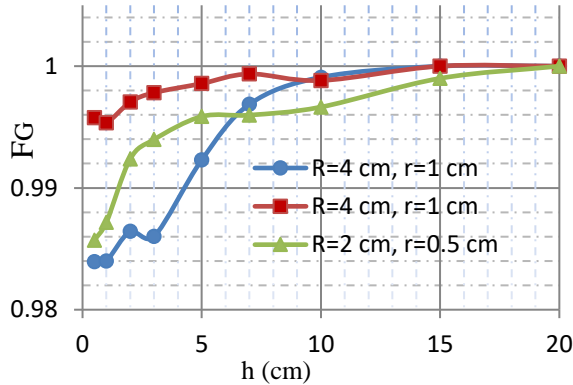


Figure 3. Geometry factors for small disk sources as function of the distance between the detector and the disk positions, h . R is the detector radius and r is the disk radius.

Assume that a small-diameter cylindrical sample with height L and located at a distance d from the detector crystal as shown in Figure 1. Two methods were considered for geometry correction factor, F_G . First method is based on the Inverse-Square Law (ISL). In this case the fraction of photons emitted from the element dx and reach the detector crystal, N_{dx} is inversely proportional to the square distance between the element dx and the detector crystal:

$$N_{dx})_{ISL} = \frac{sc}{(d+x)^2} \frac{dx}{L}, \tag{7}$$

where, the subscript ISL refers to inverse-square law, S is the source intensity and C is the proportionality constant. Therefore the number of photons per source photon reach the detector, N_s is:

$$N_s)_{ISL} = \int_0^L \frac{C}{(d+x)^2} \frac{dx}{L} = \frac{C}{d(d+L)} \tag{8}$$

Noting that according to ISL, the number of photons per source photon reach the detector from a point source located at h is:

$$N_p)_{ISL} = \frac{c}{h^2} \tag{9}$$

By dividing N_s from Eq. (8) by N_p from Eq. (9), the geometry factor F_G would be obtained:

$$F_G)_{ISL} = \frac{h^2}{d(d+L)} \tag{10}$$

The second method is based on the Solid Angle Correction (SAC) covered by the detector for the small-diameter sample (approximated to line source). The solid angle for a point source, Ω_p , located at the distance h can be calculated

from the following equation [13]:

$$\Omega_p = 2\pi \left[1 - \frac{h}{\sqrt{h^2+R^2}} \right], \tag{11}$$

where, R is the detector radius. Therefore, the solid angle for the element dx (Figure 1), Ω_{dx} at distance $d+x$ is calculated from:

$$\Omega_{dx} = 2\pi \left[1 - \frac{d+x}{\sqrt{(d+x)^2+R^2}} \right], \tag{12}$$

The solid angle for the entire sample would be:

$$\begin{aligned} \Omega_s &= 2\pi \int_0^L \left[1 - \frac{d+x}{\sqrt{(d+x)^2+R^2}} \right] \frac{dx}{L} \\ &= \frac{2\pi}{L} \left[L + \sqrt{d^2+R^2} - \sqrt{(d+L)^2+R^2} \right] \end{aligned} \tag{13}$$

Dividing Ω_s (Eq. 13) by Ω_p (Eq. 11), the geometry correction factor, F_G would be obtained:

$$F_G)_{SAC} = \frac{\sqrt{h^2+R^2}}{L(\sqrt{h^2+R^2}-h)} \left[L + \sqrt{d^2+R^2} - \sqrt{(d+L)^2+R^2} \right] \tag{14}$$

In NAA, usually the sample is measured at the sample position of the point source used in the calibration ($d = h$). Figure 4 shows the calculation results of F_G using ISL and SAC methods (Eqs. 10 and 14, respectively) and MCNPX code for 1 cm diameter samples with heights of 0.5, 1 and 2 cm. The HPGe detector used is $6^D \times 7^H$ when $d = h$. The calculations were carried out as function of the distance between the detector and the sample as shown in the figure. Table 1 gives the deviations between the analytical methods (ISI and SAC) and the Monte Carlo method. Generally, the difference between the three methods decreases with increasing the distances d and with decreasing the sample height. The SAC method is more agreeable with Monte Carlo calculations than the ISL method. At small distance d , the ISL method comes to be not reliable and should not be used.

Although, the SAC method is based on accurate analytical derivation for correction of the solid angle, a negative biasing would be observed between the SAC and Monte Carlo methods as shown in Figure 4. This error depends on the sample height and the distance between the sample and detector. This is due to that the detector intrinsic efficiency, ϵ_{int} (defined as the number of counts in full-energy peak per photon incident on the detector surface) is function of the source positions [14]. This parameter is neglected in the SAC method. The detector intrinsic efficiency of the $6^D \times 7^H$ cm HPGe detector as function of point source position, h is calculated using MCNPX code at photon energy, $E=1$ MeV as shown in Figure 5. This parameter, ϵ_{int} cannot be neglected for large samples. For example, a sample with a height of 5 cm positioned at a distance of 5 cm from the detector would have a variation of around 20% in the detector intrinsic efficiency for photons emitted from the bottom and the top of the sample.

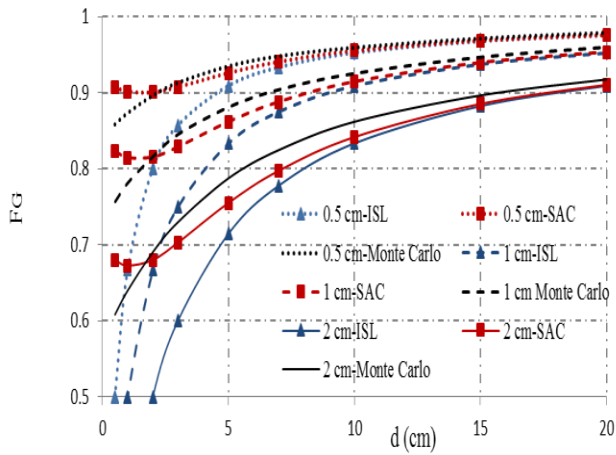


Figure 4. Calculated F_G using ISL and SAC methods and MCNPX code for 1 cm diameter samples with heights of 0.5, 1 and 2 cm when $d = h$. The HPGe detector used is $6^D \times 7^H$ cm.

Table 1. Percent deviations between the analytical methods (ISI and SAC) and the Monte Carlo method in F_G when $d = h$. The sample diameter is 1 cm and the HPGe detector is $6^D \times 7^H$ cm.

d (cm)	L=0.5 cm		L=1 cm		L=2 cm	
	ISL	SAC	ISL	SAC	ISL	SAC
0.5	-42	5.7	-56	8.7	-67	12
1	-24	3.2	-36	4.2	-48	5.2
2	-13	0.45	-18	-0.1	-26	-1.5
3	-6	-0.63	-11	-2	-18	-3.7
5	-2.7	-0.92	-5.4	-2.2	-9.3	-4.1
7	-1.5	-0.73	-3.2	-1.8	-5.7	-3.3
10	-0.67	-0.37	-1.7	-1.2	-3.3	-2.3
15	-0.30	-0.21	-0.95	-0.77	-1.6	-1.2
20	-0.26	-0.22	-0.75	-0.67	-0.90	-0.76

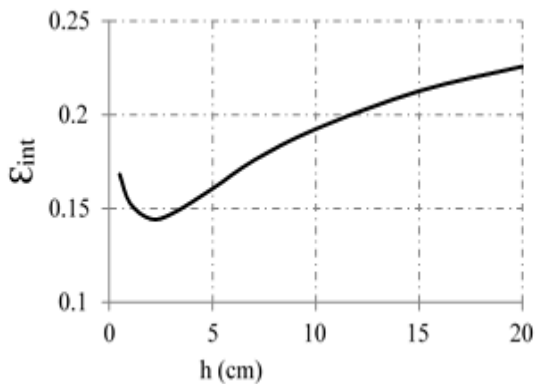


Figure 5. Intrinsic efficiency, ϵ_{int} of a $6^D \times 7^H$ cm HPGe detector as function of point source position, h at photon energy, $E=1$ MeV.

More accurate evaluation of F_G can be obtained if the point source is located at the sample center position. However, one batch of NAA samples usually has a large number of samples with different volumes and it is difficult to

calibrate the detector for each sample. In this case the position of the calibrated point source can be optimized to be near the samples centers. The above calculations were repeated assuming the point source is located at the sample center position ($h = d + L/2$). The Aguiar et al. model, Eq. (4) is included for the comparison. Fig. 6 shows the results for samples heights 1 cm and 2 cm and Table 2 gives the deviations between the analytical methods (Aguiar et al., ISL and SAC) and Monte Carlo method. As shown in the figures, the value F_G closes one for all the methods as the distance d increases and in this case detector efficiency does not need to be corrected for the sample geometry. Also, the SAC method is the most agreeable method to the Monte Carlo Method as given in Table 2.

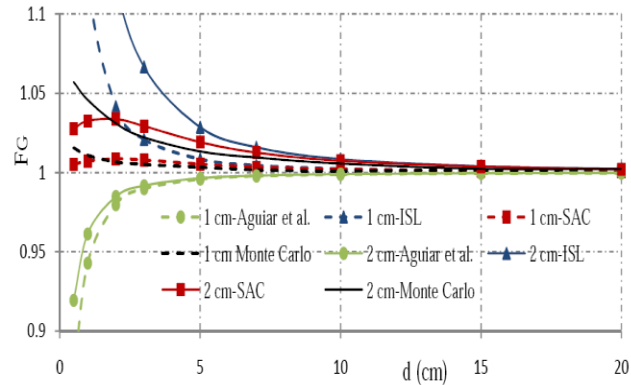


Figure 6. Calculated F_G using Aguiar et al., ISL and SAC methods and MCNPX code for 1 cm diameter samples with heights of 1 and 2 cm when $h = d + L/2$. The HPGe detector used is $6^D \times 7^H$ cm.

Table 2. Percent deviations between the analytical methods (Aguiar et al., ISI and SAC) and the Monte Carlo method in F_G when $h = d + L/2$. The sample diameter is 1 cm and the HPGe detector is $6^D \times 7^H$ cm.

d (cm)	L=1 cm			L=2 cm		
	Aguiar et al.	ISL	SAC	Aguiar et al.	ISL	SAC
0.5	-14	31	-1	-13	70	-2.8
1	-6.7	11	-0.36	-8.1	27	-1.3
2	-2.7	3.5	0.20	-4.5	9	0.26
3	-1.5	1.6	0.28	-3	4.4	0.69
5	-0.74	0.50	0.20	-1.7	1.5	0.58
7	-0.39	0.28	0.17	-1.1	0.64	0.31
10	-0.19	0.16	0.13	-0.66	0.28	0.18
15	-0.21	-0.05	-0.06	-0.29	0.15	0.13
20	-0.16	-0.07	-0.07	-0.26	-0.01	-0.01

3 Self-Attenuation Correction

To study the validity of the sample self-attenuation correction, F_μ which is derived with the assumption of parallel radiation emission, Eq. (5), three water samples with diameter of 1 cm and heights of 0.5, 1, and 2 cm have

been considered. Each sample was assumed to be measured at three different distances from a $6^D \times 7^H$ cm HPGe detector.

According to Eq. (5), F_μ is independent on the distance between the sample and the detector, d . MCNPX was used to simulate the detection system and for each case two runs were carried out. The first run is for a cylinder of vacuum and the second run is for the cylinder when it is filled with water. By dividing the detector response in the second case by its response in the first case, F_μ was calculated. Figure 7 shows F_μ as function of the photon energy for the first sample ($L=0.5$ cm) at $d=0.5, 2$ and 10 cm. The deviations between the analytical and Monte Carlo calculations are given in Table 3. Excellent agreement between the analytical and Monte Carlo calculations can be observed for all the range of photon energies (from 30 keV to 3 MeV), in particular when the distance between the detector crystal and the sample is greater than 2 cm. When the sample height is increased to 1 cm, a systematic error can be observed between the analytical and Monte Carlo calculations as shown in Figure 8. This error decreases as

Table 3. Percent deviations between the analytical method and the Monte Carlo method in F_μ calculations for samples with diameter 1 cm and heights 0.5, 1 and 2 cm. the HPGe detector is $6^D \times 7^H$ cm.

E (keV)	L = 0.5 cm			L = 1 cm			L = 2 cm		
	d=0.5 cm	d=2 cm	d=10 cm	d=2 cm	d=5 cm	d=10 cm	d=5 cm	d=10 cm	d=20 cm
30	-0.92	-0.25	0.37	1.84	1.42	0.85	5.86	2.78	0.78
60	-0.91	-0.27	0.16	1.15	0.88	0.57	3.91	2.22	1.22
100	-0.75	-0.15	0.10	0.98	0.76	0.49	3.63	2.21	1.31
200	-0.55	-0.13	0.12	0.82	0.61	0.44	2.78	1.74	1.13
500	-0.38	-0.16	0.02	0.48	0.42	0.18	1.80	1.03	0.45
1000	-0.32	-0.04	-0.14	0.33	0.43	0.14	1.28	0.97	0.52
2000	-0.30	0.25	0.26	0.56	0.40	0.30	1.47	1.20	0.66
3000	-0.09	0.10	-0.02	0.08	0.05	-0.34	0.24	-0.32	0.41

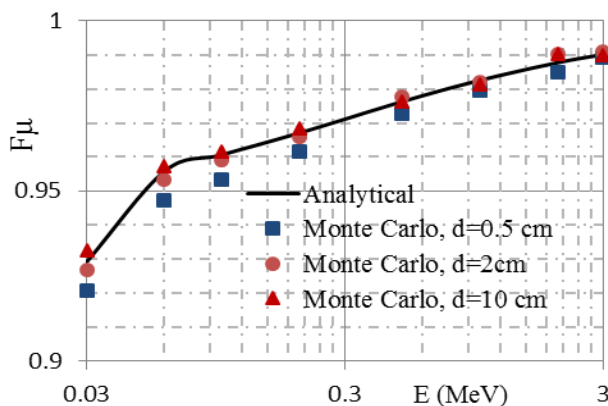


Figure 7. Analytical and Monte Carlo calculations of F_μ for $1^D \times 0.5^H$ cm sample as function of the detector energy at $d = 0.5, 2$ and 10 cm. The HPGe detector used is $6^D \times 7^H$ cm.

the photon energy, E increases and as d increases. The

deviations would be less than 1% when E is greater than 100 keV and d is greater than 2 cm as given in Table 3. When the sample is measured at $d > 10$ cm, the deviations between the analytical and Monte Carlo calculations would be less than 1% for $E > 30$ keV and less than 0.5% for $E > 100$ keV. A sample with diameter of 1 cm and height of 1 cm has a volume of 0.785 cm^3 and conventional NAA samples usually are limited to less than this volume.

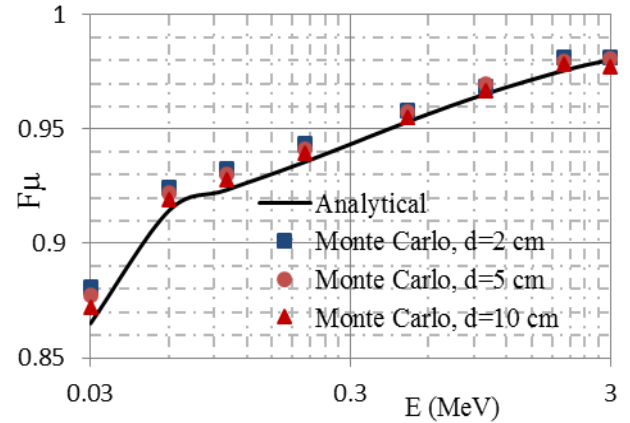


Figure 8. Analytical and Monte Carlo calculations of F_μ for $1^D \times 1^H$ cm sample as function of the detector energy at $d = 2, 5$ and 10 cm. The HPGe detector used is $6^D \times 7^H$ cm.

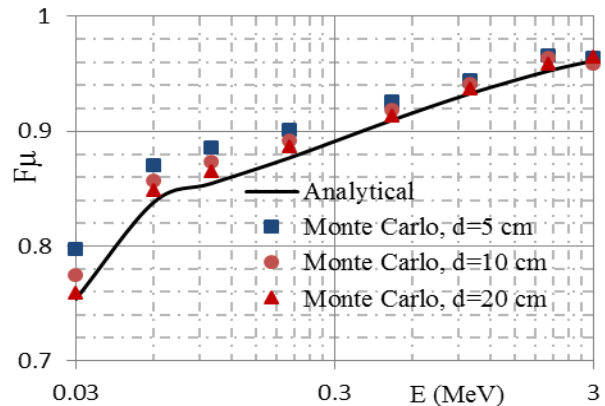


Figure 9. Analytical and Monte Carlo calculations of F_μ for $1^D \times 2^H$ cm sample as function of the detector energy at $d = 5, 10$ and 20 cm. The HPGe detector used is $6^D \times 7^H$ cm.

However, if the samples have longer heights for example $L=0.5 \rightarrow 2$, the samples should be measured at a distance far enough from the detector ($d > 20$ cm) if the approximation of parallel radiation emission is used in the calculation of sample self-attenuation correction. Figure 9 shows F_μ as function of the photon energy for the third sample ($L=2$ cm) at $d = 5, 10$ and 20 cm and the deviations between the analytical and Monte Carlo calculations are given in Table 3.

4 Experiment

A small drop of Co-60 and Eu-152 solution with activities of 2.8 and 3.5 kBq, respectively was put in a small bottle. This drop which represented the point source was counted at two positions: 10 and 10.5 cm from the crystal of a coaxial HPGe N-type Ortec detector. The detector is $7.9^D \times 9.5^H$ and has a relative efficiency of 100% and a resolution of 2.1 keV at 1.333 MeV Co-60 line. The detector is operated by Gamma Vision software. The drop was diluted to obtain a water sample with 1.2 cm in diameter (the inner diameter of the bottle) and 1 cm in height. Therefore, the new sample contains the same activities of Co-60 and Eu-152. The sample was counted at 10 cm from detector crystal. The measurement time for each run was 3.5 hrs. The first correction factor was calculated as:

$$F)_{h=d} = \frac{C_S}{C_p)_{d=h}}, \quad (15)$$

where, $F)_{h=d}$ is the full-peak efficiency correction when the drop sample and the sample are counted at the same distance from the detector, $h = d = 10$ cm, C_S is the counting rate of the sample and $C_p)_{d=h}$ is counting rate of the drop sample at $h = 10$ cm. The second correction was calculated as:

$$F)_{h=d+L/2} = \frac{C_S}{C_p)_{h=d+L/2}}, \quad (16)$$

where, $F)_{h=d+L/2}$ is the full-peak efficiency correction when the drop sample and the sample are counted at different distances, $h = d + L/2 = 10.5$ cm and $C_p)_{d=h+L/2}$ is counting rate of the drop sample at $h = 10.5$ cm. The source of uncertainty considered is the counting uncertainties:

$$\sigma_F = \sqrt{\sigma_p^2 + \sigma_s^2}, \quad (17)$$

where, σ_F is the uncertainty in the correction factor and σ_p and σ_s are the uncertainties in the drop sample and the sample counting, respectively.

MCNPX was used to simulate the detection system to calculate the two correction factors. The analytical method used to calculate the correction factors was the SAC method, Eq. (14) with the sample self-attenuation correction, Eq. (5). SAC method was selected, since it is the most accurate method with respect to the Monte Carlo calculations.

Figures 10 and 11 show the results of the three methods (Experimental, Monte Carlo and analytical calculations) for $F)_{h=d}$ and $F)_{h=d+L/2}$, respectively. The error bars are represented by the expended uncertainty (2σ). Excellent agreement between the Monte Carlo calculations and the experiment results is obtained as shown in the two figures. The deviations of the Monte Carlo and analytical calculations than the experiment results are given in Table 4. When the drop sample and the sample are counted at the same distance from the detector ($h = d = 10$ cm), a

negative biasing of the analytical method results can be observed as shown in Figure 10 and as given in Table 4. This is due to that the change of the detector intrinsic efficiency was not corrected for the volume sample as discussed above. When the drop sample is positioned at the position of the center of the volume sample ($h = d + L/2 = 10.5$ cm), the drop sample would be considered as a representative point for the sample geometry. Therefore, the deviation in the detector efficiencies for the drop sample and the sample would be due to the sample self-attenuation. In this case, the agreement between the analytical and experiment results is enhanced as shown in Figure 11 and as given in Table 4.

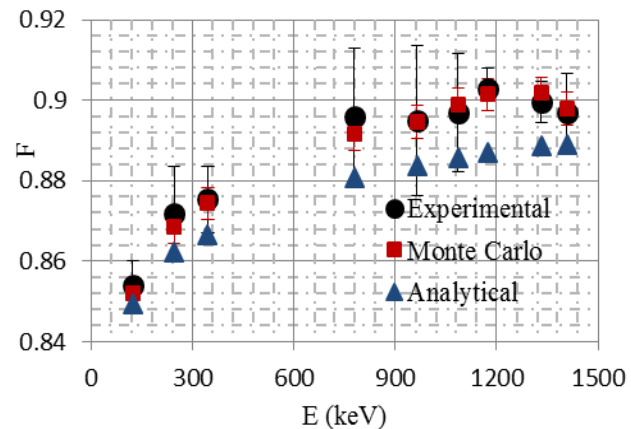


Figure 10. Experiment, Monte Carlo and analytical calculations results for $F)_{h=d}$. $d = 10$ cm, $L = 1$ cm. The HPGe detector used is $7.9^D \times 9.5^H$ cm. The error bars are represented by 2σ .

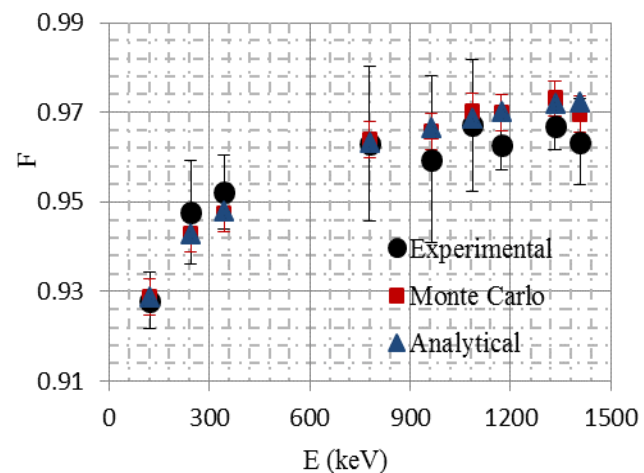


Figure 11. Experiment, Monte Carlo and analytical calculations results for $F)_{h=d+L/2}$. $d = 10$ cm, $L = 1$ cm. The HPGe detector used is $7.9^D \times 9.5^H$ cm. The error bars are represented by 2σ .

Table 4. Percent deviations of the Monte Carlo and

analytical calculations than the experiment results in F . $d = 10$ cm, $L = 1$ cm. The HPGe detector used is $7.9^D \times 9.5^H$ cm.

E (keV)	h = d		h = d + L/2	
	Monte Carlo	Analytical	Monte Carlo	Analytical
123	-0.23	-0.55	0.08	0.09
245	-0.40	-1.10	-0.51	-0.48
345	-0.11	-0.99	-0.49	-0.44
779	-0.48	-1.69	0.08	0.01
964	-0.05	-1.25	0.65	0.74
1086	0.23	-1.23	0.32	0.16
1173	-0.14	-1.75	0.75	0.78
1332	0.24	-1.20	0.65	0.54
1408	0.10	-0.87	0.64	0.93

5 Conclusion

Monte Carlo method is very accurate method of determining correction factors of HPGe detectors efficiency for NAA samples. Conventional NAA samples usually are measured far enough from the detector to minimize the coincidences. This in turn allows considering the small-diameter samples as a line source for solid angle covered by the detector determination. Eq. (14) was derived and proposed as an analytical formula for the sample geometry correction. However, determining a correction factor for the sample geometry by correcting the solid angle may lead to negative biasing, if the correction of the detector intrinsic efficiency is neglected, depending on the sample size and the distance between the detector and the sample. This problem can be overcome by positioning the calibrated point source at the position of the sample center. The approximation of parallel radiation emission in the derivation of the sample self-attenuation correction validity depends on the sample size, the distance between the sample and the detector and the photon energy.

References

- [1] I.O.B. Ewa, D. Bodizs, S. Czifrus Z. Molnar, "Monte Carlo determination of full energy peak efficiency for an HPGe detector," Appl. Radiat. Isot., 55, 103-108, 2001.
- [2] M. C. Lepy, T. Altizoglou, D. Arnold et al., "Intercomparison of efficiency transfer software for gamma-ray spectrometry," Appl. Radiat. Isot., 55, 493-503, 2001.
- [3] J.M. Laborie, G. Le Petit, D. Abt, M. Girard, "Monte Carlo calculation of the efficiency calibration curve and coincidence- summing correction in low-level gamma-ray spectrometry using well-type HPGe detectors," Appl. Radiat. Isot., 53, 57-62, 2000.
- [4] N.A.M. Mohamed, M. A. Mandour, "Evaluation of the efficiency of gamma spectrometers for measuring

volumetric samples," Nucl. Sci. Eng., 147, 185-188, 2004.

- [5] J. Saegusa, K. Kawasaki, A. Mihara, M. Ito, M. Yoshida, "Determination of detection efficiency curves of HPGe detectors on radioactivity measurements of volume samples," Appl. Radiat. Isot., 61, 1383-1390, 2004.
- [6] G. Haase, D. Tait, A. Wiechen, "Determination of full energy peak efficiency for cylindrical volume sources by the use of a point source standard in gamma-spectrometry," Nucl. Instr. and Meth. Phys. Res. A, 361, 240-244, 1995.
- [7] Z.B. Alfassi, N. Lavi, O. Presler, V. Pushkarski, "HPGe virtual point detector for radioactive disk sources," Appl. Radiat. Isot., 65, 253-258, 2007.
- [8] J.C. Aguiar, E. Galiano, J. Fernandez, "Peak efficiency calibration for attenuation corrected cylindrical sources in gamma ray spectrometry by the use of a point source," Appl. Radiat. Isot., 64, 1643-1647, 2006.
- [9] R.M.W. Overwater, P. Bode, J.J.M. Goeij, "Gamma-ray spectroscopy of voluminous sources corrections for source geometry and self-attenuation," Nucl. Instr. and Meth. Phys. Res. A, 324, 209-218, 1993.
- [10] W.R. Dixon, "Self-absorption corrections for large gamma-ray source," Nucleonics, 8, 68-72, 1951.
- [11] R.D. Evans, R.O. Evans, "Studies of self-absorption in gamma ray sources," Rev. Mod. Phys., 20, 305-326, 1948.
- [12] D.B. Pelowitz, "MCNPX user's manual, version 2.7.0," Los Alamos National Laboratory, 2011.
- [13] G.F. Knoll, "Radiation detection and measurement," third ed. Wiley, 2000.
- [14] A.A. Mowlavi, R.I. Najafabadi, R.K. Faygh, "Calculation of intrinsic efficiency of NaI(Tl) detector using MCNP code," Int. J. Pure Appl. Phys., 1, 129-136, 2005.